Ability of the Multichannel Analysis of Surface Waves Method to Resolve Subsurface Anomalies

U. Arslan[1]; J. A. Crocker[2]; J. P. Vantassel[3]; and B. R. Cox[4]

[1]Dept. of Civil, Architectural, and Environmental Engineering, Univ. of Texas Austin, Austin, TX. Email: uarslan@utexas.edu
[2]Dept. of Civil, Architectural, and Environmental Engineering, Univ. of Texas Austin, Austin, TX. Email: jcrocker@utexas.edu
[3]Dept. of Civil, Architectural, and Environmental Engineering, Univ. of Texas Austin, Austin, TX. Email: jvantassel@utexas.edu
[4]Dept. of Civil, Architectural, and Environmental Engineering, Univ. of Texas Austin, Austin, TX. Email: brcox@utexas.edu

ABSTRACT

This study examines the ability of the multichannel analysis of surface waves (MASW) method to accurately recover the size, stiffness, and depth of subsurface anomalies. The dispersion data considered in this paper were derived from waveforms generated using two-dimensional (2D) finite-difference elastic wave-propagation simulations. These simulations were performed to replicate a typical MASW field experiment on models with and without subsurface anomalies, referred to as "treatment" and "control" models, respectively. In a previously published study, the treatment and control models were compared exclusively based on differences between their experimental dispersion data to determine whether or not the anomaly could likely be detected. This study examines whether those models previously categorized as containing a detectable anomaly, based on their experimental dispersion data, can be inverted to accurately resolve the anomaly‟s size, stiffness, and depth. To rigorously perform the inversions, we adopt the procedures recommended by the surface wave inversion workflow SWinvert, which involves using multiple large-scale global-search inversions to address the problem‟s nonlinearity and multiple layering parameterizations to address the problem‟s nonuniqueness. Following the inversion process, the shear wave velocity (*Vs*) profiles from the single "best" model associated with each layering parameterization are compared to the one-dimensional (1D) *Vs* profile from the centerline of the true model using an error function to quantitatively assess the ability of the MASW method to accurately resolve subsurface anomalies. Intuitively, the ability to resolve subsurface anomalies is shown to improve as the anomaly is moved closer to the ground surface and its lateral extent increases. Surprisingly, however, in this study anomalies with lateral extents less than approximately ½ the array length located at depths >5 m most likely cannot be resolved accurately by using MASW, even when the anomalies are relatively thick (>2 m) and the impedance contrasts are notably high (>2).

INTRODUCTION

In-situ soil characterization with non-invasive surface wave methods has been widely used in past decades because they are relatively inexpensive and, perhaps erroneously presumed, easy to perform. Of these methods, the multichannel analysis of surface waves (MASW) method (Park et al., 1999; Foti, 2000) is one of the most common. Although this method is typically used to

develop one-dimensional (1D) subsurface shear wave velocity (*Vs*) profiles, an area of particular interest is the application of MASW for anomaly detection. Such applications include investigation of weak zones in levee systems (Rahimi et al., 2018), detection of karst conduits (Debeglia et al., 2006), detection of voids near the surface (i.e., < 3 m) (Nolan et al., 2011), shallow man-made tunnel detection (i.e., < 3 m) (Sloan et al., 2013), delineation of sinkholes, voids, and mines (Sloan et al., 2015; Ivanov et al., 2016) identification of the location of a dam‟s compacted core (Hock et al., 2007), and evaluation of unknown subsurface bridge foundations (Mahvelati and Coe, 2017). The successful application of surface wave methods for anomaly detection relies on the anomaly being within the vertical and horizontal detection limits, which depend on a number of factors, including: (a) the receiver spacing and length of the MASW array, (b) the minimum and maximum frequencies/wavelengths resolved during testing, (c) the size of the anomaly, and (d) the stiffness contrast of the anomaly relative to the surrounding materials (Xia et al., 1999; Park, 2005; Ivanov et al., 2008). However, successful *detection* of an anomaly at the dispersion processing stage does not necessarily equal successful *resolution* of the anomaly during the inversion stage. Accurately resolving subsurface anomalies can be challenging for surface wave methods due to: (1) the 1D nature of the forward problem used to calculate theoretical dispersion curves from a trial subsurface model, whereas anomalies inherently induce 2D/3D variability in the subsurface, and (2) the non-uniqueness of surface wave inversion, which results in a number of candidate models that can fit the experimental data equally well.

In this paper, we consider synthetic subsurface models developed in a previous study by Crocker et al. (2020). The development of these models began with a simple uniform body of soil (half-space) containing no anomalies. These control models were developed with a constant mass density (ρ) and Poisson„s ratio (v) for *Vs* values of 150 and 300 m/s. Then, anomalies with various combinations of size (lateral extent and thickness), stiffness, and depth were placed into the control models to produce treatment models (refer to Figure 1a). These anomalies were created to be either softer or stiffer than the surrounding half-space using several different impedance contrasts (the ratio between the anomaly *Vs* to the half-space *Vs*). For example, a treatment model with an anomaly impedance contrast of 2.0 and a half-space with *Vs* equal to 150 m/s contains an anomaly with *Vs* equal to 300 m/s. Approximately 3,000 different treatment models were developed in this manner.

Following model development, Crocker et al. (2020) used a 2D finite-difference program (Köhn et al., 2012) to simulate wave propagations for MASW experiments at the surface of models with and without anomalies. As shown in Figure 1a, several different shot locations were used for each model and the simulated waveforms were recorded using a 24-channel MASW array with 1-m spacing between receivers (total array length of 23 m). The simulated wavefields were then processed using the frequency domain beamformer method (Zywicki and Rix, 2005) to obtain dispersion data. The dispersion data from the treatment and control models were compared quantitatively using a dispersion misfit function (i.e., L1 norm of residuals between the mean treatment and control experimental dispersion data, normalized by the control model‟s uncertainty). The obtained misfit, which we will hereafter refer to unambiguously as the relative dispersion misfit ($M_{dc,rel}$), was then used to categorize anomalies as likely detectable (i.e., $M_{dc,rel} > 1$) or likely non-detectable (i.e., $M_{dc,rel} < 1$). To provide a convenient reference, the results from similar models were synthesized into figures such as that shown in Figure 1b, which for a given impedance contrast (IC), anomaly thickness (T), and half-space velocity (*Vs,hs*), the user could assess the range of relative dispersion misfits as a function of the anomaly's lateral extent normalized by the MASW array length (LE/AL; abscissa) and the anomaly's top depth (ordi-

nate). For example, Figure 1b shows $M_{dc,rel}$ for models with IC = 5.0, T = 2 m, and Vs,hs = 150 m/s. As mentioned previously, a $M_{dc,rel}$ value of 1.0 was considered as the boundary between models containing anomalies that were, and were not, likely detectable, and is indicated for reference with a thin white line in Figure 1b.

Due to the complexity and computational expense of surface wave inversion, through the course of this study, we inverted only 120 of the nearly 3,000 treatment models developed by Crocker et al. (2020). Models were selected to encompass various anomaly thicknesses, LE/AL ratios (noting that AL = 23 m was constant for all models discussed herein), depths, and impedance contrasts to observe the influence of each factor on anomaly resolution. We focused primarily on models that were likely detectable based on high $M_{dc,rel}$ (i.e., > 1), and therefore the most likely to be resolvable, however, some models with low $M_{dc,rel}$ (i.e., < 1) were also inverted to verify this assumption. To synthesize the most interesting results of the inversion study, this paper will only focus on two model trends. The first trend involves treatment models with increasing LE/AL ratios and constant thickness, depth, half-space velocity, and impedance contrast (such as those indicated by black circles in Figure 1b). The second trend involves treatment models with increasing depth to the top of the anomaly and constant LE/AR ratios, thickness, half-space velocity, and impedance contrast.

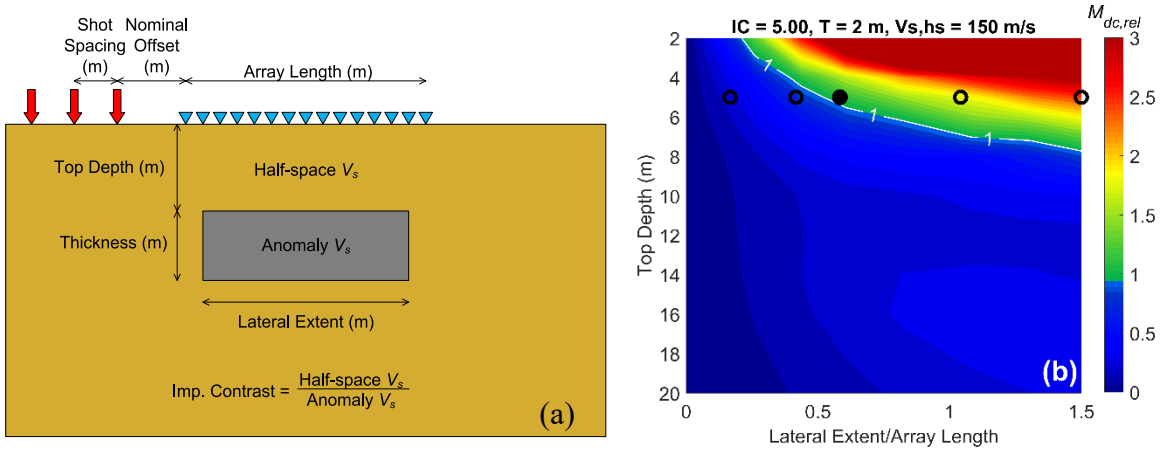

Figure 1. (a) Schematic of a treatment model, and (b) summary of relative dispersion misfits ($M_{dc,rel}$) from Crocker et al. (2020) for treatment models with an impendence contrast (IC) of 5, thickness (T) of 2 m, and half-space shear wave velocity (Vs,hs) of 150 m/s. Black circles at a top depth of 5 m indicate the treatment models selected for inversion to explore the effect of the anomalies' lateral extent/array length (LE/AL) ratio.

INVERSION METHODOLOGY

Before discussing the details of our inversion methodology, we offer a brief summary of surface wave inversion. The purpose of surface wave inversion is to find the 1D subsurface model(s) with layer thicknesses (H), *Vs*, compression wave velocity (*Vp*), and mass density (ρ) whose solution to the analytical forward problem (i.e., theoretical dispersion curve) best matches the experimental dispersion data. Of particular importance is the determination of the subsurface *Vs* profile, as it has the greatest sensitivity in the forward problem and importance in engineering practice. To assess the goodness-of-fit between a potential model"s theoretical dispersion curve, as calculated through the forward problem (Thomson, 1950; Haskell, 1953), and the

experimental dispersion data, inversion requires the definition of a dispersion misfit (M_{disp}). M_{disp} is most typically a L2 norm of error, or some normalized version thereof. In order to minimize M_{disp} (i.e., find the best match between a candidate model‟s theoretical dispersion curve and the experimental dispersion data), various inversion algorithms have been proposed to alter the model properties. Once a model has been found whose theoretical dispersion curve closely matches the experimental dispersion data, it can be inferred that the model, and most importantly its *Vs* profile, is an acceptable representation of the subsurface. However, this process is not unique.

To rigorously invert the 120 sets of experimental dispersion data selected from Crocker et al. (2020), we adopt the surface wave inversion workflow SWinvert, developed by Vantassel and Cox (2020). This workflow entails using multiple large-scale global-search inversions to address the inverse problem‟s non-linearity and multiple parameterizations to consider non-uniqueness in the subsurface layering. The implementation details of this workflow are explained in the following sections.

INVERSION TUNING PARAMETERS

The inversions in this study were performed using the open-source tool SWbatch (Vantassel et al., 2020), which enables users to perform batch-style surface wave inversions that consider multiple trials to explore the inverse problem‟s non-linearity, and multiple layering parameterizations to explore its non-uniqueness, as required by the SWinvert workflow. Since these inversions can become computationally expensive, SWbatch has been developed into an easy-to-use web-application on the DesignSafe-CI (Rathje et al., 2017) workspace to allow users with no knowledge of high-performance computing to gain its benefits in their research. SWbatch is built upon the global-search Neighborhood Algorithm developed by Sambridge (1999) and implemented for surface-wave inversion in the Dinver module (Wathelet et al., 2004) of the open-source software Geopsy (Wathelet et al., 2020).

We invert each set of experimental dispersion data from the 120 treatment models considered using five different layering parameterizations (discussed next), each with five different inversion trials. For each trial inversion, we search 150,000 models, such that we consider 750,000 models in total for each layering parameterization (i.e., 150,000 models per trial and 5 trials per parameterization). To select a single answer for comparison with the true solution, we select the “best” (i.e., lowest misfit) model out of the 750,000 models for each layering parameterization. Because using such a large number of trial models is computationally expensive, we reduce some of the computational expense by resampling the experimental dispersion data prior to inversion using 20-30 points in log-frequency space (Vantassel and Cox, 2020).

INVERSION PARAMETERIZATION

Developing inversion parameterizations is a crucial part of the inversion process to obtain reliable results (Cox and Teague, 2016; DiGiulio et al., 2012). The range of the parameterization (e.g., upper and lower limit on *Vs*) must be broad enough to include the true model, but also relatively restricted such that reasonable results are produced and needless time is not spent searching areas of the parameter space that do not contain the true model. As mentioned previously, the treatment and control models were developed to have a constant ρ and ν with variable *Vs* and layer thicknesses. As such, the focus in this study is the inversion parameterization of *Vs* and the

number of trial layers. To consistently parameterize *Vs* across all treatment models considered, we select a range of twice the highest *Vs* and half of the lowest *Vs* based on the true model. For example, for an IC of 5.0 and a *Vs,hs* of 150 m/s, the *Vs* of the anomaly would be 750 m/s, and therefore the chosen *Vs* inversion parameterization range was set at 75 (= 0.5*150) to 1,500 (= 2*750) m/s. While knowledge of the true *Vs* profile is untenable in practice, as the true model is never known, we do so here to ensure the parameterization contains the true model and avoid the time consuming process of iteratively adjusting the inversion parameterization, as is typically required in practice. We do not apply any limitations on the change in *Vs* (and *Vp,* discussed later) between layers. Furthermore, we do not constrain the velocity of any given layer to be faster than the layer above it, thereby allowing for the detection of soft anomalies and/or the detection of soft layers below stiff anomalies. This general approach of enabling velocity reversals in all trial layers is common practice when inverting dispersion data to detect subsurface anomalies. To parameterize layer thicknesses, we utilize Layering by Number‟s (LN) of 3, 4, and 5 and fixed-thickness layers (FTL) of 10 and 20. The LN parameterization is discussed at length in Vantassel and Cox (2020), but for the edification of the reader a brief summary is provided here. An LN=5, for example, divides the subsurface into 5 layers, including the half-space. The minimum thickness of each layer is controlled by the minimum experimental dispersion data wavelength (λ) divided by 3, while the maximum profile depth is controlled by dividing the maximum experimental dispersion data λ by a depth factor (df), which is taken as 2 in this study to satisfy the recommendations of Foti et al. (2018). In contrast, the FTL approach parameterizes a profile with a set number of layers of equal/fixed thickness. FTL=10, for example, includes 10 layers of equal thickness between the surface and the maximum profile depth, defined in the same manner as that for LN. Of note to the reader, both approaches are programmed in SWprepost (Vantassel, 2020), an open-source Python package for surface-wave inversion pre- and post-processing, such that these (and other) parameterizations can be generated programmatically and exported directly to the .param format used by Dinver.

While not the primary focus of attention here, the parameterization of *Vp* and mass density also deserve a brief discussion. The range of *Vp* for all layers was defined as twice the *Vs* range (i.e., 150 to 3,000 m/s for the example discussed above), while the *Vp* layer thicknesses were defined using an LN=3, regardless of the *Vs* layering parameterization. Mass density was always held constant at the true density of 2,000 kg/m^3. Poisson‟s ratio, while not a true inversion parameter (as it is uniquely determined by *Vs* and *Vp*), is used by Dinver as an additional constraint available to the user to ensure the consistency of the *Vs* and *Vp* during inversion. Poisson‟s ratio was parameterized with an LN=1 and allowed to vary between 0.15 and 0.5.

To ensure reasonable results and expedite convergence to a good solution, the parameter ranges for both *Vp* and *Vs* were adjusted for the near-surface layers by interpreting the experimental dispersion data on a case-by-case basis. To illustrate the parameterization adjustment procedure, Figure 2a shows the experimental dispersion data from one treatment model in terms of frequency. The phase velocity is observed to be nearly constant at approximately 140 m/s between 30 to 100 Hz, which corresponds to wavelengths between 1 and 5 m ($\lambda=V/f$). Because the resolution depth can be approximated as λ/df, where df is 2 or 3, we can assert that a uniform soil layer exists between 2 to 3 m. This allows us to then narrow the default velocity parameterization range in the upper 2 to 3 m from 75-1,500 m/s to a more reasonable, but still quite conservative, 75-250 m/s.

A DETAILED PRESENTATION OF A SINGLE EXAMPLE

Before presenting the full results, we first discuss a single example to illustrate a few important points. Figure 2a shows the experimental dispersion data for the example treatment model in terms of frequency. The example model is composed of a *Vs,hs* of 150 m/s and an anomaly with a T of 2 m, LE/AL = 0.61 (i.e., LE = 14 m), top depth of 5 m, and *Vs* of 750 m/s (i.e., IC=5). As noted above, this model is indicated in Figure 1b by the solid black symbol, which has a relative dispersion misfit greater than 1 (meaning it is likely detectable). The 1D *Vs* profile at the middle of the treatment model is shown as the solution in Figure 2b. Figure 2a also shows the single "best"/lowest misfit theoretical dispersion curves from each of the five considered inversion parameterizations. Qualitatively, the theoretical dispersion curves are all observed to fit the experimental data extremely well across all frequencies. This qualitative assessment is confirmed quantitatively by the low dispersion misfit values (M_{disp} < 0.25), indicating an excellent fit between the theoretical dispersion curves and the experimental dispersion data. However, Figure 2b shows that the *Vs* profiles corresponding to these theoretical dispersion curves, which match the experimental dispersion data so precisely, poorly capture the anomaly‟s thickness and velocity, despite the LN parameterizations doing a fair job of capturing the anomaly‟s top depth. To assess the agreement between the true solution (i.e., the 1D *Vs* profile at the center of the model) and the best 1D *Vs* profile determined during inversion, and to further compare the best 1D *Vs* profiles obtained from different layering parameterizations, we calculate the model‟s *Vs* misfit (M_{Vs}) using the normalized L1 of residuals, proposed by Vantassel and Cox (2020). M_{Vs} is described in Equation 1:

$$M_{Vs} = \frac{1}{N}\sum_{i=1}^{N}\frac{|Vs_{i,inversion} - Vs_{i,solution}|}{Vs_{i,solution}} \quad (1)$$

where N is the total number of depth discretizations, $Vs_{i,inversion}$ is the *Vs* of the best inversion result at depth i, and $Vs_{i,solution}$ is the *Vs* of the solution model at depth i. For this study, 0.1 m intervals were used to discretize the profiles from 0 to 20 m depth. The M_{Vs} values for the profiles shown in Figure 2b illustrate quantitatively that the LN parameterizations (M_{Vs} between 0.19 and 0.39) well outperform their FTL counterparts (M_{Vs} between 1.33 and 2.8), resulting in better estimates of the site‟s subsurface. However, this is not to imply that the LN parameterizations do a "good" job resolving the anomaly, as none of the parameterizations are able to capture both the anomaly's thickness and velocity. This comparison does, however, indicate that parameterizing an inversion using a large number of thin layers does not guarantee better resolution of subsurface anomalies (a common misconception) and is more likely to introduce spurious subsurface layering despite fitting the experimental dispersion data quite well (e.g., FTL=10).

DISCUSSION OF MANY INVERSION RESULTS

We now present the inversion results pertaining to the two categories of interest for this paper, which include the effects of: (1) increasing anomaly lateral extent, and (2) increasing top depth to the anomaly. We begin with the effect of increasing lateral extent. Figure 3 summarizes the inversion results for a model with *Vs,hs* of 150 m/s and an anomaly with a T of 2 m, top depth of 5 m, *Vs* of 750 m/s, and five different LE/AL ratios. Figure 3a illustrates that the $M_{dc,rel}$ for the five lateral extents (black circles) increases from approximately 0.3 (unlikely detectable) at LE/AL = 0.17 (4 m LE) to 2.5 (likely detectable) at LE/AL = 1.56 (36 m LE). We now assess

whether these anomalies can be accurately resolved using MASW inversions. Figures 3b-f show the inversion results for increasing LE/AL ratios. We observe qualitatively (i.e., visually assessing the *Vs* profiles) and quantitatively (i.e., comparing M_{Vs}) that as the lateral extent increases [i.e., proceed from (b) to (f)], the quality of the *Vs* resolution for the reasonable parameterizations (i.e., LN) generally improves. However, it is important to note that this improvement is not monotonic with increasing LE/AL ratio (due to a number of complicating factors discussed later), but only a general improving trend from poor resolution at LE/AL = 0.17 (Figure 3b) to better resolution at LE/AL = 1.56 (Figure 3f). Importantly, while we note that the anomaly resolution improves with increasing lateral extent, this is not to say that any of the anomalies (even the one with the largest lateral extent) is well-resolved, but rather that anomalies with limited lateral extent are much less well-resolved. From this set of examples, we conclude that the MASW method is unlikely to accurately resolve subsurface anomalies when they have small LE/AL ratios (less than ~ 0.5), even when the anomalies are located relatively close to the ground surface (top depth of 5 m) and are relatively thick (2 m). Furthermore, for anomalies with LE/AL > 0.5 MASW is better able to resolve the anomaly‟s thickness and top depth, but remains unable to reliably resolve the anomaly‟s velocity.

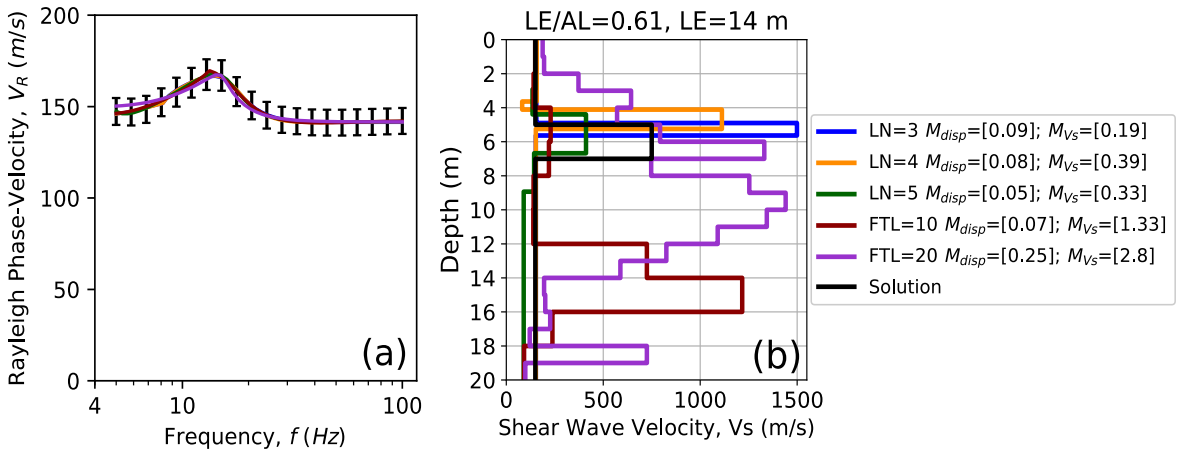

Figure 2. Experimental dispersion data in terms of (a) frequency for a treatment model with a half-space velocity (*Vs,hs*) of 150 m/s and an anomaly with a thickness (T) of 2 m, lateral extent of 14 m (i.e., LE/AL = 0.61), top depth of 5 m, and velocity of 750 m/s (i.e., IC=5). The *Vs* profiles resulting from the inversion of experimental dispersion data in panel (a) are shown in panel (b). Misfit values between theoretical and experimental dispersion data (M_{disp}) and between inverted and true solution *Vs* profiles (M_{Vs}) for each LN and FTL parameterization are indicated in the legend.

We now examine the effect of increasing anomaly top depth, or moving the anomaly deeper into the control model. Figure 4 summarizes the inversion results for a model with a *Vs,hs* of 300 m/s and an anomaly with a T of 4 m, LE/AL ratio of 0.61, *Vs* of 600 m/s (i.e., IC=2), and five different top depths. Figure 4a from Crocker et al. (2020) illustrates that the $M_{dc,rel}$ for the five models (black circles) decrease from 2.8 (likely detectable) at 2 m top depth to 0.4 (unlikely detectable) at 10 m top depth. The inversion results used to investigate anomaly top depths of 2, 4, 5, 8, and 10 m are presented in Figures 4b-f. A comparison of the results confirms that the ability to resolve an anomaly deteriorates as its depth increases. However, the results follow a

less clear and consistent pattern due to the compounding impact of the lateral extent, which at 14 m is just slightly above the LE/AL > 0.5 threshold for likely anomaly resolution, as discussed previously. Yet, despite these complicating factors, we observe that for those anomalies closer to the surface (top depth < 5 m), the reasonable parameterizations (i.e., LNs) are generally able to recover the anomaly‟s top depth, although they are unable to consistently recover its thickness and velocity. Whereas those models with deeper anomalies (top depth > 5 m) are unable to even recover the anomaly‟s top depth. From this example, we observe that the ability to resolve a sub-surface anomaly decreases as its top depth increases, as anticipated. In particular, we find for this example with a lower IC, that the MASW method is unable to accurately resolve the thickness and velocity of the anomaly at any top depth, despite the anomaly being of considerable size (4 m thick and 14 m lateral extent).

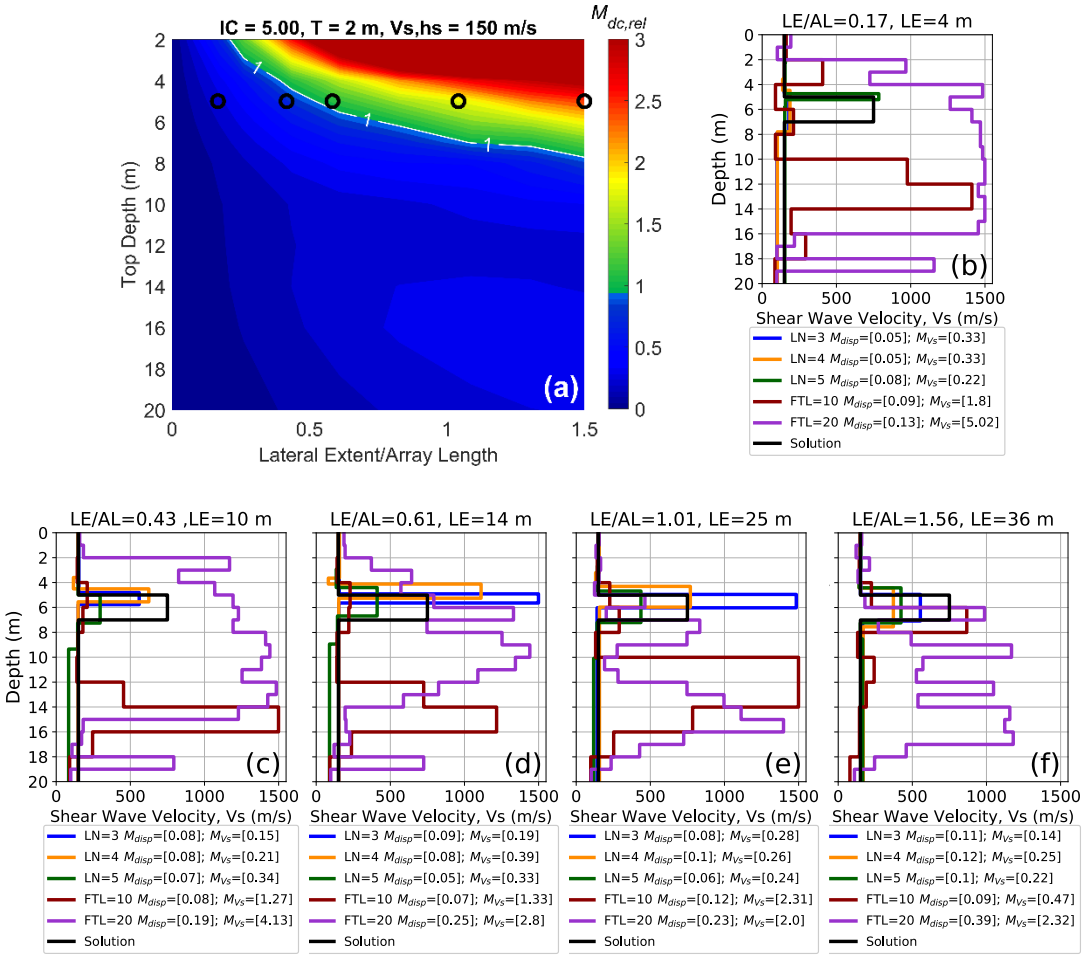

Figure 3. (a) Summary of relative dispersion misfit ($M_{dc,rel}$) for a model with half-space velocity (Vs,hs) of 150 m/s and an anomaly with a thickness of 2 m, top depth of 5 m, Vs of 750 m/s (IC=5), and five different LE/AL ratios. (b) – (f) present the inversion results for models with anomalies with lateral extents equal to 4, 10, 14, 25, and 36 m, respectively. These models are further indicated by black circles on Figure 3a. Misfit values between theoretical and experimental dispersion data (M_{disp}) and between inverted and true solution Vs profiles (M_{Vs}) for each LN and FTL parameterization are indicated in the legend.

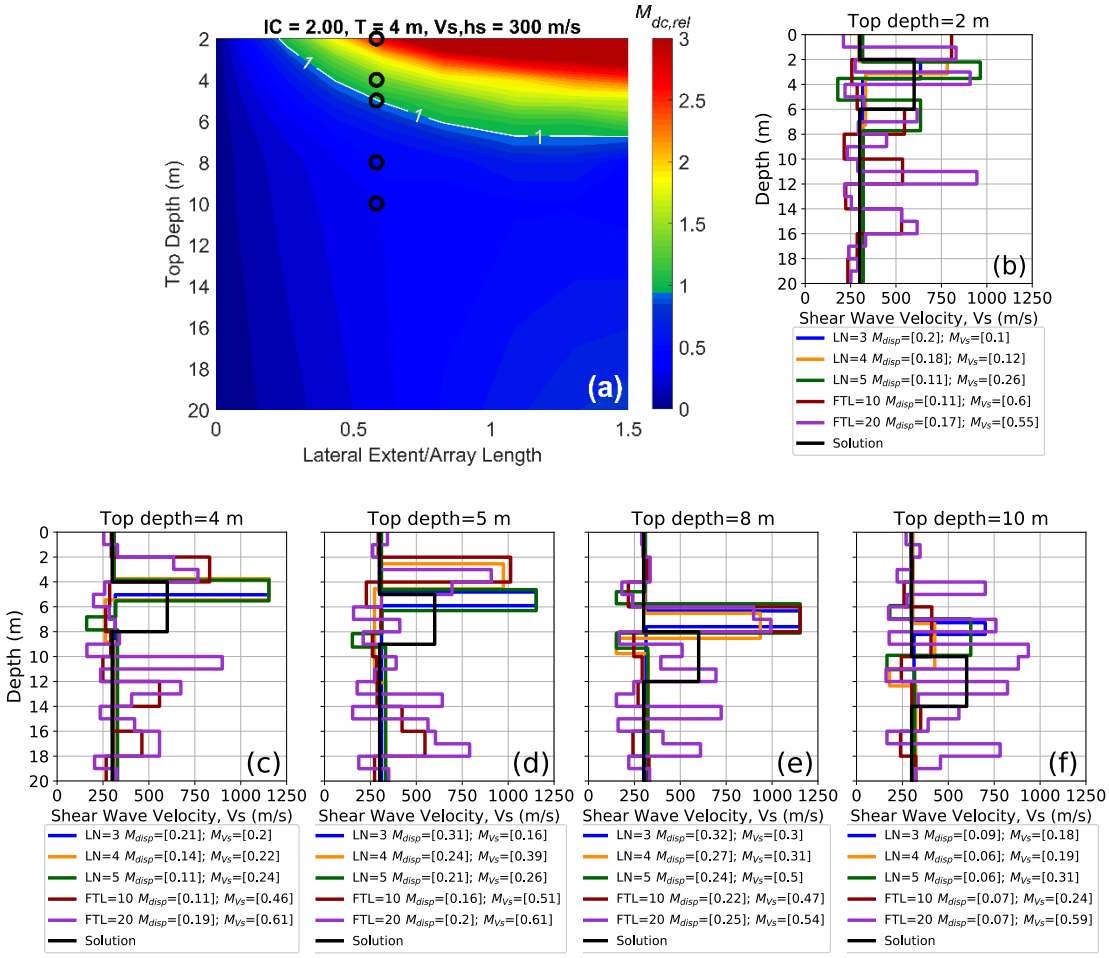

Figure 4. (a) Summary of relative dispersion misfit ($M_{dc,rel}$) for a model with half-space velocity (Vs,hs) of 300 m/s and an anomaly with a thickness of 4 m, Vs of 600 m/s (IC=2), lateral extent of 14 m (i.e., LE/AL = 0.61), and five different top depths. (b) – (f) present the inversion results for models with anomalies with top depths equal to 2, 4, 5, 8, and 10 m, respectively. These models are further indicated by black circles in panel (a). Misfit values between theoretical and experimental dispersion data (M_{disp}) and between inverted and true solution Vs profiles (M_{Vs}) for each LN and FTL parameterization are indicated in the legend.

CONCLUSIONS

This study examines the ability of the MASW method to accurately recover the size, stiffness, and depth of subsurface anomalies. The dispersion data considered in this paper were derived from waveforms generated using 2D finite-difference elastic wave-propagation simulation on models with and without subsurface anomalies, referred to as "treatment" and "control" models, respectively. In a previously published study, the treatment and control models were compared exclusively based on differences between their experimental dispersion data to determine whether or not the anomaly could likely be *detected*. This study examines whether those models previously categorized as containing a detectable anomaly based on their experimental disper-

sion data can be inverted to accurately *resolve* the anomaly‟s size, stiffness, and depth. In particular we focus on the effect of: (1) increasing anomaly lateral extent, and (2) increasing anomaly top depth on the resulting agreement between the 1D true solution *Vs* profiles (as defined at the center of the true model) and the inversion-derived *Vs* profiles from multiple parameterizations. The ability to resolve subsurface anomalies is shown to improve as the anomaly‟s lateral extent increases and as the anomaly moves closer to the ground surface. However, while the MASW method was able to reasonably recover the top depth and thickness of anomalies with large lateral extents (LE/AL > ~ 0.5), it was unable to accurately recover their velocity. In addition, as models with sufficient lateral extent were moved deeper into the model, MASW loses even its ability to accurately recover the anomaly‟s top depth and thickness. This is despite the fact that the anomalies presented were relatively thick (> 2 m) and with a significant impedance contrast (> 2) to the surrounding medium.

ACKNOWLEDGEMENTS

All inversions were performed using the DesignSafe-CI (Rathje et al., 2017) application SWbatch (Vantassel et al., 2020). To handle the large amount of results produced through the course of this study SWprepost (Vantassel, 2020), an open-source Python package, was used for all surface-wave inversion pre- and post-processing. Author U.A. would like to thank the General Directorate of State Hydraulic Works (DSI) and the Republic of Turkey for supporting him in this research. Additionally, this material is based upon work supported by the National Science Foundation (NSF) Graduate Research Fellowship Program under Grant No. DGE – 1610403 and NSF Grant CMMI-1931162. Any opinions, findings, and conclusions or recommendations expressed in this material are those of the authors and do not necessarily reflect the views of NSF.

REFERENCES

Cox, B. R., and Teague, D. P. (2016). Layering ratios: A systematic approach to the inversion of surface wave data in the absence of a priori information. *Geophysical Journal International*, 207(1), 422–438.

Crocker, A. J., Ugur, A., Vantassel, J., and Cox, B. (2020). Limitations of the multichannel analysis of surface waves (MASW) method for subsurface anomaly detection. Accepted to the *6th International Conference on Geotechnical and Geophysical Site Characterization* in Budapest, Hungary. 7-11 September 2020 (postponed to 2021 due to COVID-19).

Debeglia, N., Bitri, A., and Thierry, P. (2006). Karst investigations using microgravity and MASW; application to Orléans, France. *Near Surface Geophysics*, 4(4), 215–225.

Di Giulio, G., Savvaidis, A., Ohrnberger, M., Wathelet, M., Cornou, C., Knapmeyer-Endrun, B., and Bard, P. Y. (2012). Exploring the model space and ranking a best class of models in surface-wave dispersion inversion: Application at European strong-motion sitesExploring model space, ranking best models. *Geophysics*, 77(3), B147-B166.

Foti, S. (2000). *Multistation methods for geotechnical characterization using surface waves*. Politecnico Di Torino Ph D Dissertation, 42, 315–323.

Foti, S., Hollender, F., Garofalo, F., Albarello, D., Asten, M., Bard, P.-Y., Comina, C., Cornou, C., Cox, B., Di Giulio, G., Forbriger, T., Hayashi, K., Lunedei, E., Martin, A., Mercerat, D., Ohrnberger, M., Poggi, V., Renalier, F., Sicilia, D., and Socco, V. (2018). "Guidelines for the good practice of surface wave analysis: a product of the InterPACIFIC project." *Bulletin of Earthquake Engineering*, 16(6), 2367–2420.

Haskell, B. N. A. (1953). The dispersion of surface waves on multilayered media. 43(1), 17–34.

Hock, S., Ivanov, J., and Miller, R. D. (2007). Test for detecting an impermeable water barrier in an earth-fill dam in Austria using MASW method. *Proceedings of the Symposium on the Application of Geophyics to Engineering and Environmental Problems*, SAGEEP, 1, 610–617.

Ivanov, J., Miller, R., and Peterie, S. (2016). Detecting and delineating voids and mines using surface-wave methods in Galena, Kansas. In *SEG Technical Program Expanded Abstracts 2016* (pp. 2344-2350). Society of Exploration Geophysicists.

Ivanov, J., Miller, R. D., and Tsoflias, G. (2008, April). Some practical aspects of MASW analysis and processing. In *21st EEGS Symposium on the Application of Geophysics to Engineering and Environmental Problems* (pp. cp-177). European Association of Geoscientists & Engineers.

Köhn, D., De Nil, D., Kurzmann, A., Przebindowska, A., and Bohlen, T. (2012). On the influence of model parametrization in elastic full waveform tomography. *Geophysical Journal International*, 191(1), 325-345.

Mahvelati, S., and Coe, J. T. (2017). The use of two dimensional (2D) Multichannel Analysis of Surface Waves (MASW) testing to evaluate the geometry of an unknown bridge foundation. *Geotechnical Special Publication*, 2012(GSP 277), 657–666.

Nolan, J. J., Sloan, S. D., Broadfoot, S. W., Mckenna, J. R., and Metheny, O. M. (2011). Near-surface void identification using MASW and refraction tomography techniques. In *SEG Technical Program Expanded Abstracts 2011* (pp. 1401-1405). Society of Exploration Geophysicists.

Park, C. B. (2005). MASW horizontal resolution in 2D shear-velocity (Vs) mapping. Open-File Report, Lawrence: Kansas Geologic Survey.

Park, C. B., Miller, R. D., and Xia, J. (1999). Multichannel analysis of surface waves. *Geophysics*, 64(3), 800–808.

Rahimi, S., Wood, C. M., Coker, F., Moody, T., Bernhardt-Barry, M., and Mofarraj Kouchaki, B. (2018). The combined use of MASW and resistivity surveys for levee assessment: A case study of the Melvin Price Reach of the Wood River Levee. *Engineering Geology*, 241(April), 11–24.

Rathje, E. M., Dawson, C., Padgett, J. E., Pinelli, J. P., Stanzione, D., Adair, A., Arduino, P., Brandenberg, S. J., Cockerill, T., Dey, C., Esteva, M., Haan, F. L., Hanlon, M., Kareem, A., Lowes, L., Mock, S., and Mosqueda, G. (2017). DesignSafe: New Cyberinfrastructure for Natural Hazards Engineering. *Natural Hazards Review*, 18(3), 1–7.

Sambridge, M. (1999). *Geophysical inversion with a neighbourhood algorithm — I. Searching a parameter space*. 479–494.

Sloan, S. D., Nolan, J. J., Broadfoot, S. W., McKenna, J. R., and Metheny, O. M. (2013). Using near-surface seismic refraction tomography and multichannel analysis of surface waves to detect shallow tunnels: A feasibility study. *Journal of Applied Geophysics*, 99, 60-65.

Sloan, S. D., Schwenk, J. T., Stevens, R. H., and Butler, B. W. (2015, November). Hazard assessment and site characterization at an oil and gas well site using surface wave methods. In *International Conference on Engineering Geophysics*, Al Ain, United Arab Emirates, 15-18 November 2015 (pp. 114-117). Society of Exploration Geophysicists.

Thomson, W. T. (1950). Transmission of elastic waves through a stratified solid medium. *Journal of Applied Physics*, 21(2), 89–93.

Vantassel, J. P. (2020) jpvantassel/swprepost: latest (Concept).

Vantassel, J. P., Gurram, H., and Cox, B. R. (2020) jpvantassel/swbatch: latest (Concept).

Vantassel, J. P., and Cox, B. R. (2020). SWinvert: A workflow for performing rigorous surface wave inversions. 1–25. http://arxiv.org/abs/2005.11820.

Wathelet, M., Jongmans, D., and Ohrnberger, M. (2004). Surface-wave inversion using a direct search algorithm and its application to ambient vibration measurements. *Near Surface Geophysics*, 2(4), 211–221.

Wathelet, Marc, Chatelain, J. L., Cornou, C., Giulio, G., Di, Guillier, B., Ohrnberger, M., and Savvaidis, A. (2020). Geopsy: A user-friendly open-source tool set for ambient vibration processing. *Seismological Research Letters*, 91(3), 1878–1889.

Xia, J., Miller, R. D., and Park, C. B. (1999). Estimation of near-surface shear-wave velocity by inversion of Rayleigh waves. *Geophysics*, 64(3), 691-700.

Zywicki, D. J., and Rix, G. J. (2005). Mitigation of near-field effects for seismic surface wave velocity estimation with cylindrical beamformers. *Journal of geotechnical and geoenvironmental engineering*, 131(8), 970-977.